Static and Dynamic Single-Crystal X-ray Diffraction Studies of Some Solid-State Photodimerization Reactions

Hachiro Nakanishi, William Jones,* John M. Thomas,*

Department of Physical Chemistry, University of Cambridge, Cambridge, CB2 1EP England

Michael B. Hursthouse,* and Majid Motevalli

Department of Chemistry, Queen Mary College, London, E1 4NS England *(Received: April 6, 1981)*

A class of diffusionless photochemical reactions involving (2 + 2) photodimerization in the solid state is described. The archetypal molecule, 2-benzyl-5-benzylidenecyclopentanone (BBCP), and its *p*-bromo derivative (BpBrBCP) crystallize into space groups and unit cells which permit single-crystal → single-crystal transformations to occur. Detailed crystallographic studies of these materials at various stages of solid-state conversion at room temperature are described. In particular, for the case of BBCP, the "formation" of the cyclobutane ring between the two monomers in an incipient dimer can be directly identified by using dynamic four-circle diffractometry. Full structural and related details are presented.

Introduction

The detailed mechanism by which organic reactions proceed within the solid state is not completely understood although there is cogent evidence to suggest that for certain photoinduced and thermally induced reactions the nature and stereochemistry of the product is precisely determined by the crystal packing within the perfect monomer lattice.[1] Noteworthy examples of this so-called topochemical control include the photodimerization of cinnamic acids,[2] the 2 + 2 polymerization of distyrylpyrazine and analogues,[3] and the polymerization of several diacetylene derivatives.[4] In all these cases the reaction proceeds under strict topochemical control to yield product, the molecular symmetry of which is predetermined by the symmetry existing within the reacting crystal matrix.

Furthermore, recent progress in analyzing the crystal-packing forces which dictate the overall crystal structure adopted by a molecular species[5] has permitted the design of molecules in which particular symmetries of reaction site may be produced within the reacting monomer lattice (see, for example, the use of dichloro substitution as a means of aligning molecules within stacks to enable photodimerization of mixed crystals to occur).[6]

To date, however, no system has allowed a detailed study of the course of such photoinduced dimerization or polymerization transformations,[7] and, therefore, little progress has been possible firstly in determining the mechanism by which crystal → crystal reactions proceed and secondly in rationalizing those features which are important for controlling both the crystallinity of product and the topotactic relationship between reactant and product. (At first sight, the well-known polymerizable *p*-toluenesulfonate derivative of diacetylene[4] seems to offer ideal scope for the detailed crystallographic study of a solid-state reaction by X-ray methods. This solid, however, reacts too rapidly to permit the satisfactory collection of intensity data on a four-circle diffractometer at intermediate stages of conversion. Moreover with the diacetylenes as a family it has so far not proved feasible to quell the photoreaction by a suitable reduction in temperature as this often results in phase changes that generate low-temperature stable phases within which topochemical reactions cannot proceed.)

Scheme I

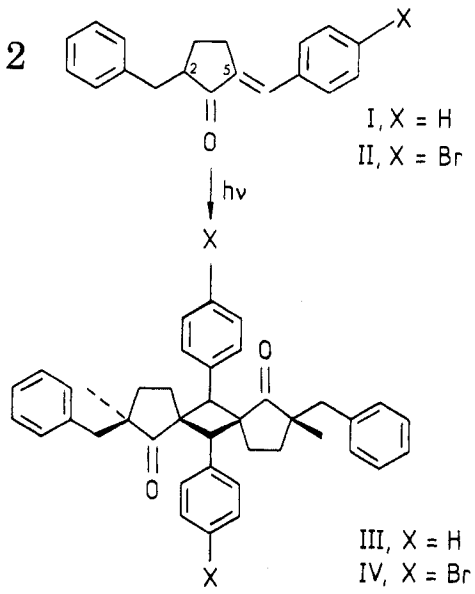

In this paper, we describe the first detailed X-ray crystallographic study of a photochemically induced single-crystal → single-crystal reaction and show how it is possible to monitor the variation in cell parameters and structure factor amplitudes, and obtain structural data for partially converted material. These detailed studies are

(1) G. M. J. Schmidt, *Pure Appl. Chem.*, **27**, 647 (1971); J. M. Thomas, *Phil. Trans. R. Soc. London*, **277**, 251 (1974); *Pure Appl. Chem.*, **51**, 1065 (1979); M. D. Cohen and B. S. Green, *Chem. Brit.*, **9**, 490 (1973); J. M. Thomas, S. E. Morsi, and J. P. Desvergne, *Adv. Phys. Org. Chem.*, **15**, 63 (1977).

(2) G. M. J. Schmidt in "Reactivity of the Photo-excited Organic Molecule", Interscience, New York, 1967.

(3) M. Hasegawa, M. Iguchi, and H. Nakanishi, *J. Polym. Sci., A1*, **6**, 1054 (1968); H. Nakanishi, W. Jones, J. M. Thomas, M. Hasegawa, and W. L. Rees, *Proc. R. Soc. London, Ser. A*, **369**, 307 (1980).

(4) G. Wegner, *Z. Naturforsch. B*, **24**, 824 (1969); R. Baughman, *J. Appl. Phys.*, **43**, 4362 (1972); *J. Chem. Phys.*, **68**, 3110 (1978).

(5) A. I. Kitaigorodskii in "Molecular Crystals and Molecules", Academic Press, London, 1973; J. M. Thomas and W. Jones, 6th International Symposium on Reactivity of Solids, Sept 1980, Cracow, in press.

(6) A. Elgavi, B. S. Green, and G. M. J. Schmidt, *J. Am. Chem. Soc.*, **95**, 2058 (1973).

(7) The recently described work by R. Popovitz-Biro et al. (*Pure Appl. Chem.*, in press) relates to the dynamic study of the reaction between host and guest within a deoxycholic acid/acetophenone complex and presents an important study of the molecular rotations associated with chemical reactions.

0022-3654/81/2085-3636$01.25/0

TABLE I: Crystal Data, Intensity Data, Collection Parameters, and Details of Refinement

	BpBrBCP	BBCPM	BBCP30	BBCP70	BBCPD
			Crystal Data		
a, Å	34.222 (6)	31.302 (11)	31.310	31.300 (4)	31.321 (4)
b, Å	10.923 (1)	10.784 (3)	10.761	10.780 (2)	10.811 (4)
c, Å	8.427 (1)	8.687 (3)	8.741	8.735 (2)	8.629 (3)
space group	*Pbca*	*Pbca*	*Pbca*	*Pbca*	*Pbca*
V, Å^3	3150	2932	2945.1	2947.3	2921.8
Z	8	8	(8)	(4)	4
D_c, g cm^{-3}	1.44	1.19	1.18	1.18	1.19
$F_{(000)}$	1392	1120	1120	1120	1120
radiation			Ni filtered, Cu Kα, λ = 1.5418 Å		
μ, cm^{-1}	37.4	4.79	4.77	4.76	4.81
			Data Collection		
crystal size, mm^3	0.15 × 0.2 × 0.2	0.1 × 0.15 × 0.2		0.5 × 0.37 × 0.12	0.67 × 0.45 × 0.10
$\theta_{min}/\theta_{max}$	3,75	3,70	3,65	3,65	3,65
scan mode	$\omega/2\theta$	$\omega/2\theta$	$\omega/2\theta$	$\omega/2\theta$	$\omega/2\theta$
scan speed	4° min^{-1}	4° min^{-1}	variable	variable	variable
scan width, deg			0.9 + 0.3 tan θ	0.9 + 0.3 tan θ	0.7 + 0.3 tan θ
horizontal aperture, mm			4.0	4.0	4.0
vertical aperture, mm			4.0	4.0	4.0
total data measured	2879	2926	2959	2968	2580
total data unique	2737	2513	2507	2504	2485
total data observed	2005	1340	1069	1140	1676
significance test	$F_o > 5\sigma(F_o)$	$F_o > 5\sigma(F_o)$	$F_o > 3\sigma(F_o)$	$F_o > 3\sigma(F_o)$	$F_o > 3\sigma(F_o)$
			Refinement		
no. of parameters	258	253	199	199	250
weighting scheme			unit weights		
final $R = \Sigma(\Delta F)/\Sigma(F_o)$	0.059	0.057	0.146	0.138	0.058

based on the solid-state photodimerization of 2-benzyl-5-benzylidenecyclopentanone (BBCP, I) and 2-benzyl-5-*p*-bromobenzylidenecyclopentanone (BpBrBCP, II) (Scheme I).

Preliminary accounts of some of the salient features of the solid-state photodimerization of BpBrBCP and BBCP have been described and, in particular, the dimerization of both I and II shown to be of single-crystal → single-crystal transformations.[8,9] To obtain a deeper understanding of the processes which control the production of crystalline dimer (BBCPD, III, and BpBrBCPD, IV) and which may also control the crystallinity (or otherwise) of other dimerization and polymerization reactions we have used a four-circle diffractometer to study the change from monomer → dimer for I and II. In addition, we have determined the hitherto unreported crystal structures of I, II, and III. The crystal structure of IV was published by Whiting.[10]

Experimental Section

(i) *Preparative Details.* BBCP and BpBrBCP were prepared following the method described by Forward and Whiting.[11] Single crystals were obtained from chloroform–methanol mixtures [BBCP, colorless plates, mp 124.5–125.5 °C (lit., yellow plates, mp 126–127 °C); BpBrBCP, colorless plates, mp 135–136 °C (lit., yellow plates, mp 132–133 °C)].

The dimer of BBCP was prepared by irradiation of monomer dispersed in a water–methanol (2:1) mixture maintained at ca. 10 °C with UV light, filtered such that λ > 320 nm. Melting point and infrared analysis confirmed that conversion to dimer was complete (dimer mp 236–238 °C; lit.[11] mp 242.5–243.5 °C). Slow crystallization of dimer from a methanol–chloroform mixture resulted in the formation of a solvate (cell parameters: a = 25.47, b = 6.15, c = 21.48 Å; β = 121.4°; space group $C2/c$). Precipitation, however, resulted in very small crystals of the solvent-free dimer, the cell parameters of which were close to those found for the as-dimerized crystals (see later). Warming of the crystals of the solvate to remove solvent resulted in the destruction of single-crystal character.

(*ii*) *X-ray Studies.* (*a*) *Photographic Recording.* Weissenberg and oscillation photographs were taken with Ni-filtered Cu Kα radiation. For the study of topotaxy (i.e., the mutual crystallographic relationships between the unit cell axes of the parent and daughter phases), plated-shaped crystals were mounted on a goniometer head and oscillation and Weissenberg photographs taken at various stages of reaction. For BBCP, reaction was induced by means of a 100-W medium-pressure mercury lamp filtered such that λ > 320 nm, the crystal being rotated continuously during conversion. For BpBrBCP, it was found that exposure to room daylight provided a suitably slow conversion rate and yielded single crystals of product without disintegration of the reacting crystal.

(*b*) *Four-Circle Measurements. Structural Investigations.* Complete sets of intensity data were recorded for BBCP monomer (BBCPM, I) and dimer (BBCPD, III), BpBrBCP monomer (II), and also for a crystal of BBCP at two intermediate points (approximately 30%, BBCP30, and 70%, BBCP70) on the monomer → dimer conversion curve.

For BBCPM, the data were collected on a Phillips four-circle diffractometer, for BpBrBCP on a Syntex $P2_1$, and for BBCPD and BBCP30 and BBCP70 on a Nonius CAD4, following previously described procedures.[12,13] Details of the crystal data and intensity measurement are summarized in Table I. The structure of BpBrBCP was

(8) H. Nakanishi, W. Jones, and J. M. Thomas, *Chem. Phys. Lett.*, **71**, 44 (1980).
(9) W. Jones, H. Nakanishi, C. R. Theocharis, and J. M. Thomas, *J. Chem. Soc., Chem. Commun.*, 610 (1980); H. Nakanishi, W. Jones, J. M. Thomas, M. B. Hursthouse, and M. Motevalli, *ibid.*, 611 (1980).
(10) D. A. Whiting, *J. Chem. Soc. C*, 3396 (1971).
(11) G. C. Forward and D. A. Whiting, *J. Chem. Soc. C*, 1868 (1969).
(12) H. Nakanishi, C. R. Theocharis, and W. Jones, *Acta Crystallogr.*, in press.
(13) M. B. Hursthouse, R. A. Jones, K. M. A. Malik, and G. Wilkinson, *J. Am. Chem. Soc.*, **101**, 4128 (1979).

TABLE II: Fractional Atomic Coordinates ($\times 10^4$) for BBCPM with Esd's in Parentheses

	x	y	z
O(1)	426 (1)	2377 (3)	128 (4)
C(1)	417 (1)	3229 (4)	1071 (5)
C(2)	803 (1)	3756 (4)	1850 (5)
C(3)	647 (1)	5010 (4)	2377 (5)
C(4)	174 (1)	4897 (4)	2678 (5)
C(5)	31 (1)	3823 (3)	1686 (4)
C(6)	1216 (1)	3655 (4)	994 (5)
C(7)	1605 (1)	3912 (4)	1955 (5)
C(8)	1782 (2)	3032 (5)	2909 (6)
C(9)	2130 (2)	3287 (6)	3801 (6)
C(10)	2315 (1)	4426 (7)	3755 (7)
C(11)	2148 (2)	5314 (5)	2808 (7)
C(12)	1797 (1)	5060 (5)	1944 (6)
C(13)	−352 (1)	3364 (3)	1391 (4)
C(14)	−777 (1)	3690 (3)	1951 (4)
C(15)	−854 (1)	4587 (4)	3091 (5)
C(16)	−1259 (2)	4813 (4)	3590 (5)
C(17)	−1599 (2)	4198 (5)	3004 (6)
C(18)	−1533 (1)	3321 (5)	1866 (6)
C(19)	−1131 (1)	3081 (4)	1376 (5)
H(C2)	874 (10)	3169 (23)	2749 (27)
H(C3)1	795 (11)	5333 (24)	3188 (26)
H(C3)2	686 (11)	5593 (24)	1508 (27)
H(C4)1	−12 (11)	5658 (23)	2494 (26)
H(C4)2	124 (10)	4658 (23)	3796 (26)
H(C6)1	1217 (10)	2768 (23)	596 (26)
H(C6)2	1188 (11)	4375 (24)	120 (27)
H(C8)	1656 (11)	2302 (24)	2956 (27)
H(C9)	2275 (10)	2655 (25)	4471 (26)
H(C10)	2564 (12)	4685 (24)	4352 (26)
H(C11)	2307 (10)	6164 (24)	2681 (27)
H(C12)	1680 (11)	5646 (24)	1357 (26)
H(C13)	−342 (10)	2677 (24)	720 (26)
H(C15)	−627 (11)	5002 (23)	3470 (26)
H(C16)	−1283 (11)	5351 (24)	4365 (26)
H(C17)	−1890 (11)	4363 (24)	3316 (26)
H(C18)	−1792 (11)	2908 (23)	1470 (26)
H(C19)	−1068 (10)	2494 (25)	592 (26)

TABLE III: Fractional Atomic Coordinates ($\times 10^4$) for BBCPD with Esd's in Parentheses

	x	y	z
O(1)	488 (1)	2701 (2)	153 (3)
C(1)	507 (1)	3614 (3)	957 (3)
C(2)	858 (1)	3854 (4)	2138 (4)
C(3)	712 (1)	5054 (4)	2919 (4)
C(4)	230 (1)	5102 (4)	2701 (4)
C(5)	178 (1)	4640 (3)	1009 (3)
C(6)	1295 (1)	3815 (5)	1395 (5)
C(7)	1656 (1)	4093 (4)	2503 (4)
C(8)	1842 (1)	5248 (5)	2510 (6)
C(9)	2174 (2)	5567 (7)	3442 (7)
C(10)	2328 (2)	4675 (10)	4434 (9)
C(11)	2154 (2)	3501 (9)	4482 (7)
C(12)	1819 (2)	3202 (5)	3496 (6)
C(13)	−250 (1)	4301 (3)	239 (3)
C(14)	−662 (1)	4210 (3)	1103 (4)
C(15)	−795 (1)	5074 (4)	2228 (4)
C(16)	−1197 (2)	4956 (6)	2896 (5)
C(17)	−1467 (2)	4023 (6)	2479 (6)
C(18)	−1340 (2)	3165 (5)	1386 (7)
C(19)	−945 (1)	3260 (4)	741 (5)
H(2)	914 (11)	3065 (32)	2809 (43)
H(31)	805 (12)	5094 (35)	3908 (44)
H(32)	846 (11)	5873 (33)	2538 (43)
H(41)	77 (10)	4547 (28)	3291 (35)
H(42)	99 (10)	6092 (31)	2897 (38)
H(61)	1271 (14)	4512 (41)	573 (52)
H(62)	1315 (11)	2876 (35)	1021 (43)
H(8)	1721 (14)	5946 (40)	1942 (51)
H(9)	2333 (17)	6685 (50)	3320 (60)
H(10)	2565 (19)	4874 (58)	4858 (67)
H(11)	2224 (16)	2852 (48)	5019 (60)
H(12)	1644 (12)	2391 (39)	3420 (48)
H(13)	−195 (9)	3461 (26)	−219 (32)
H(15)	−569 (10)	5776 (29)	2500 (37)
H(16)	−1262 (13)	5655 (37)	3516 (47)
H(17)	−1773 (14)	3911 (37)	2756 (48)
H(18)	−1558 (13)	2463 (43)	1182 (50)
H(19)	−824 (12)	2663 (38)	148 (46)

solved by the heavy atom method and BBCPM (I) and BBCPD (III) by direct methods. The structures were refined by least squares with all non-hydrogen atoms assigned anisotropic temperature factors. For BBCPM and BBCPD, hydrogen atoms were included and refined with isotropic temperature factors. For the mixed crystals various refinement procedures were tried in attempts to find the best models for the crystal structures and these are discussed later; for these two structures hydrogen atom contributions were included by using the riding model. Details of the basic refinements for all five structures are given in Table I. For all structures, scattering factors were taken from ref[14]. All structure determination computations were made by using SHELX[15a] and diagrams prepared by using PLUTO 78[15b] or ORTEP[15c] on the Cambridge IBM 370, QMC ICL 2980, and ULCC CDC 7600 computers. Atomic coordinates for the pure phases are given in Tables II–IV. Those for the mixed phases, along with all lists of thermal parameters and F_o/F_c values are available as supplementary material. (See paragraph at end of text regarding supplementary material.)

Dynamic Investigations. Appropriate single crystals of BBCPM and BpBrBCP were selected for each study and irradiated, in situ, on a Nonius CAD4 diffractometer. At the commencement of each experiment, and after each irradiation, cell dimensions were determined by least-squares refinement of setting angles for 23 automatically centered reflections. Intensity data were also recorded for these reflections as well as for an additional 20, so that the variation of diffraction intensity with conversion could be monitored. The reflections were chosen by reference to the intensities recorded for the pure monomer and dimer phases, so that some would show increases, some decreases, and some no changes in intensity throughout the reactions. After each irradiation, profiles for θ and ω scans were recorded for three well-separated reflections in order to monitor any changes in mosaic spread and to check whether any fracturing had occurred.

Results and Discussion

(*i*) *Dynamical Investigation of Transformation.* (*a*) *Photographic Recording.* Oscillation and Weissenberg (*hk*0) photographs obtained from a sample of monomer BBCP irradiated for 65.5 h showed very little change, although careful measurement indicated that slight changes in cell dimensions had occurred, along with changes in intensity of some reflections. The retention of crystalline and morphological integrity of the sample was established by optical microscopy. Melting point measurement (236–238 °C) confirmed that the crystal was now essentially dimeric.

For BpBrBCP the increased reactivity of this material compared with the larger changes in cell parameters associated with the conversion resulted in the necessity for much slower conversion rates for crystal integrity to be preserved. However, provided sufficient care was taken, it was still possible to obtain a single-crystal → single-

(14) "International Tables for X-ray Crystallography", Vol. III, Kynoch Press, Birmingham, 1962.

(15) (a) G. M. Sheldrick, program for crystal structure determination, University of Cambridge, England, 1976. (b) C. K. Johnson, ORTEP Report ORNL-3794, Oak Ridge National Laboratory, Oak Ridge, TN, 1965. (c) W. D. S. Motherwell, PLUTO, University of Cambridge, 1978.

TABLE IV: Fractional Atomic Coordinates for BpBrBCP ($\times 10^4$ for C, O and Br; $\times 10^3$ for H) with Esd's in Parentheses

	x	y	z
O(1)	−641 (1)	2582 (4)	5425 (5)
C(1)	−649 (2)	1779 (5)	4430 (7)
C(2)	−1010 (2)	1271 (6)	3674 (8)
C(3)	−881 (2)	89 (6)	2940 (8)
C(4)	−446 (2)	150 (5)	2675 (7)
C(5)	−304 (2)	1190 (5)	3705 (6)
C(6)	−1377 (2)	1368 (7)	4618 (8)
C(7)	−1733 (2)	860 (6)	3775 (8)
C(8)	−1958 (2)	1587 (7)	2798 (10)
C(9)	−2271 (2)	1073 (10)	1979 (10)
C(10)	−2364 (2)	−145 (9)	2119 (11)
C(11)	−2139 (2)	−835 (8)	3091 (11)
C(12)	−1838 (2)	−365 (7)	3912 (9)
C(13)	52 (2)	1661 (5)	3927 (7)
C(14)	431 (2)	1363 (5)	3245 (7)
C(15)	499 (2)	330 (5)	2257 (8)
C(16)	859 (2)	131 (6)	1618 (7)
C(17)	1168 (2)	896 (5)	1900 (7)
C(18)	1109 (2)	1914 (6)	2880 (8)
C(19)	750 (2)	2120 (5)	3542 (7)
BR(1)	1656 (0)	611 (1)	968 (1)
H(C2)	−107 (2)	197 (4)	276 (4)
H(C3)1	−92 (2)	−36 (4)	359 (4)
H(C3)2	−107 (2)	−23 (4)	200 (4)
H(C4)1	−40 (2)	24 (4)	169 (4)
H(C4)2	−32 (2)	−59 (4)	290 (4)
H(C6)1	−129 (2)	78 (4)	563 (4)
H(C6)2	−140 (2)	227 (4)	500 (4)
H(C8)	−190 (2)	248 (4)	267 (4)
H(C9)	−240 (2)	163 (4)	150 (4)
H(C10)	−267 (2)	−32 (4)	164 (4)
H(C11)	−216 (2)	−171 (4)	311 (4)
H(C12)	−167 (2)	−80 (4)	449 (4)
H(C13)	6 (2)	234 (4)	457 (4)
H(C15)	29 (2)	−14 (4)	204 (4)
H(C16)	91 (2)	−42 (4)	105 (4)
H(C18)	130 (1)	241 (4)	311 (4)
H(C19)	71 (2)	274 (4)	415 (4)

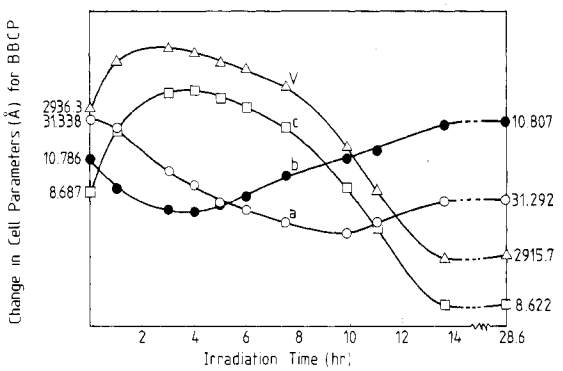

Figure 1. Diagram of the variation in cell parameters for BBCP.

crystal transformation, even though those crystals which were slowly converted still showed some evidence of cracking.

(*b*) *Four-Circle Measurements.* Because the parameters of the monomer and dimer for BBCP are very similar it was necessary, in order to follow clearly the change in cell parameters with conversion, to perform the experiment in situ on a four-circle diffractometer. Table IX shows the variation in the cell parameters during the course of the conversion.[16] Peak profile analysis showed that ω half-widths increased typically from 0.25 to 0.37° during the conversion. Figure 1 illustrates the variation in cell parameters and associated volume during the transformation

(16) The measured intensities for certain of the reflections have been deposited.

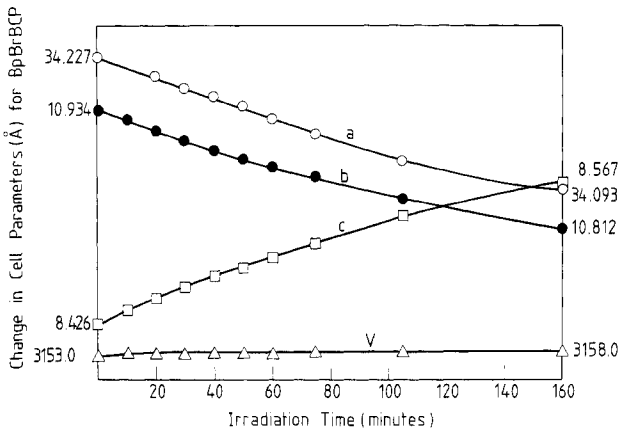

Figure 2. Diagram of the variation in cell parameters for BpBrBCP.

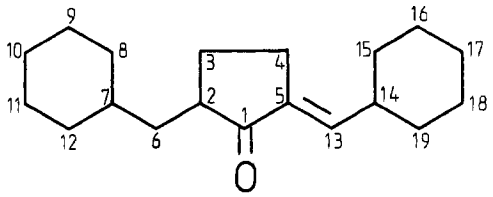

Figure 3. Molecule of BBCPM showing atom numbering scheme.

of BBCP. The changes are seen to be smooth and continuous, although they do not vary in a simple manner throughout the reaction; *c* and *V* initially increase whereas *b* initially decreases. The variation in *a* is slightly more uniform. In all cases the final values are, within experimental limits, similar to those obtained from the crystal used for structural work on BBCP dimer. Reproducibility of the nature of the cell parameters variation was confirmed with two other crystals, although it was noticed that the absolute values of fully dimerized specimens (and indeed the monomers to a certain extent) was variable and clearly specimen dependent. In the case of the dimers, we are confident that size variation was a real effect and not an indication of monomer impurity (cf. also crystal data table).

In the case of BpBrBCP (II) the more pronounced change in cell parameters between monomer and dimer, combined with the increased rate of reaction when compared to BBCP, means that a single-crystal → single-crystal transformation will result only during very slow conversion, otherwise strain tends to shatter the parent matrix. That a single-crystal to single-crystal transformation is possible is shown by Weissenberg X-ray photographs. For the four-circle work, however, it was not possible, because of the long times required, to irradiate sufficiently slowly and, therefore, even with our slowest rates, after partial conversion the crystal cracked. Before this stage was reached, however, the conversion followed a smooth path (Figure 2) similar to that seen for BBCP, suggesting perhaps that the transformation mechanisms for BBCP and BpBrBCP are broadly similar.

(*ii*) *Structural Investigations.* (*a*) *Pure Structures.* The final atomic coordinates for all structures are given in Table II–IV. A molecule of BBCPM is shown in Figure 3, which also defines the atomic numbering scheme used for all structures; for the dimer species, centrosymmetrically related atoms are denoted by (atom)′.

Bond lengths and angles for the three pure phase are given in Table V–VII. For the monomers the relatively short single bonds C(1)–C(5) (BBCP, 1.469(5); BpBrBCP, 1.477(5) and C(13)–C(14) (1.459(5); 1.456(5)) indicates that π-electron delocalization is operative throughout the car-

TABLE V: Bond Lengths (Å) and Angles (Deg) for BBCPM

O(1)-C(1)	1.231 (4)	C(8)-C(9)	1.366 (7)
C(1)-C(2)	1.495 (5)	C(9)-C(10)	1.357 (8)
C(1)-C(5)	1.469 (5)	C(10)-C(11)	1.367 (7)
C(2)-C(3)	1.508 (5)	C(11)-C(12)	1.358 (6)
C(2)-C(6)	1.495 (5)	C(13)-C(14)	1.457 (5)
C(3)-C(4)	1.511 (5)	C(14)-C(15)	1.406 (5)
C(4)-C(5)	1.510 (5)	C(14)-C(19)	1.382 (5)
C(5)-C(13)	1.323 (5)	C(15)-C(16)	1.361 (6)
C(6)-C(7)	1.502 (6)	C(16)-C(17)	1.353 (6)
C(7)-C(8)	1.376 (6)	C(17)-C(18)	1.383 (7)
C(7)-C(12)	1.375 (6)	C(18)-C(19)	1.352 (6)
O(1)-C(1)-C(2)	124.6 (4)	C(7)-C(8)-C(9)	121.6 (5)
O(1)-C(1)-C(5)	125.8 (4)	C(8)-C(9)-C(10)	120.4 (5)
C(2)-C(1)-C(5)	109.5 (3)	C(9)-C(10)-C(11)	119.2 (5)
C(1)-C(2)-C(3)	102.6 (3)	C(10)-C(11)-C(12)	120.1 (5)
C(1)-C(2)-C(6)	116.4 (3)	C(7)-C(12)-C(11)	122.1 (5)
C(3)-C(2)-C(6)	119.6 (4)	C(5)-C(13)-C(14)	132.2 (3)
C(2)-C(3)-C(4)	107.2 (3)	C(13)-C(14)-C(15)	124.0 (3)
C(3)-C(4)-C(5)	104.6 (3)	C(13)-C(14)-C(19)	119.8 (4)
C(1)-C(5)-C(4)	107.4 (3)	C(15)-C(14)-C(19)	116.3 (4)
C(1)-C(5)-C(13)	120.9 (3)	C(14)-C(15)-C(16)	120.5 (4)
C(4)-C(5)-C(13)	131.7 (3)	C(15)-C(16)-C(17)	121.7 (5)
C(2)-C(6)-C(7)	114.3 (4)	C(16)-C(17)-C(18)	119.1 (4)
C(6)-C(7)-C(8)	122.3 (4)	C(17)-C(18)-C(19)	119.7 (5)
C(6)-C(7)-C(12)	121.1 (4)	C(14)-C(19)-C(18)	122.8 (4)
C(8)-C(7)-C(12)	116.6 (4)		

bonyl, ethylene groups, and the benzene ring (C(14)–C(19)). This part of the two molecules is relatively planar, the maximum deviation from the mean plane being 0.14 Å at C(14) for BBCP and 0.12 Å for BpBrBCP. The molecules as a whole, however, are not planar and the benzene ring C(17)–C(12) makes dihedral angles of 73.0(3) and 69.0(5)° with the mean planes for BBCP and BpBrBCP, respectively. In the crystal, the molecules are so oriented that their long axis is nearly parallel to the *a* axis and consequently perpendicular to the (100) plane (Figure 4). As expected from the isomorphous nature of the two structures the principal packing modes are the same, the molecules forming incipient dimer pairs across centers of symmetry (see Figure 3). The intermolecular distances between double bonds within these dimeric units are 4.166(5) and 3.798(9) Å respectively and consequently upon UV irradiation it is these pairs which react topochemically to yield centrosymmetric photodimers. The

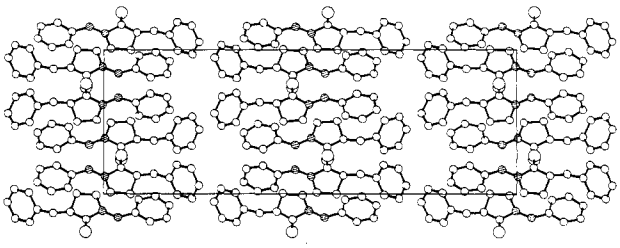

Figure 4. Packing diagram of BBCPM viewed along [001]. The atoms comprising the ethylenic groups are hatched for clarity.

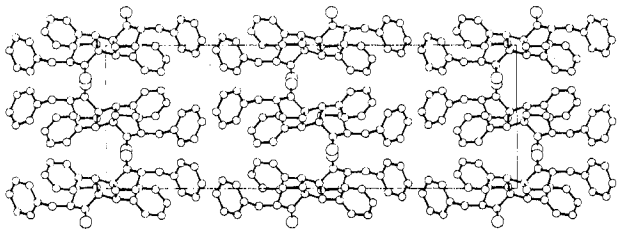

Figure 5. Packing diagram of BBCPD viewed along [001].

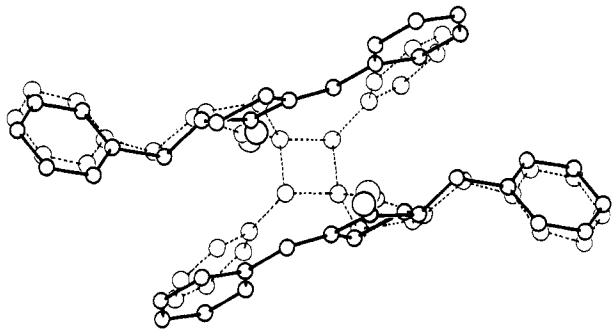

Figure 6. Composite diagram comparing the packing of the molecular units within the monomer and dimer crystal structures.

value of 3.798(9) Å found for BpBrBCP is among the smallest so far found for solid-state photocycloaddition reactions[2,3] and comparison with the value of 4.166(8) Å for BBCP suggests that the greater reactivity of BpBrBCP compared with BBCP may be interpretable in terms of a simple distance–reactivity correlation. A similar tendency has been found for the topochemical photopolymerization

TABLE VI: Bond Lengths (Å) and Angles (Deg) for BBCPD

C(1)-O(1)	1.208 (6)	C(2)-C(1)	1.520 (6)
C(5)-C(1)	1.515 (6)	C(3)-C(2)	1.531 (7)
C(6)-C(2)	1.514 (7)	C(4)-C(3)	1.520 (7)
C(5)-C(6)	1.552 (6)	C(13)-C(5)	1.541 (6)
C(7)-C(6)	1.511 (7)	C(8)-C(7)	1.377 (7)
C(12)-C(7)	1.387 (7)	C(9)-C(8)	1.359 (7)
C(10)-C(9)	1.378 (10)	C(11)-C(10)	1.382 (11)
C(12)-C(11)	1.388 (9)	C(14)-C(13)	1.494 (5)
C(15)-C(14)	1.409 (6)	C(19)-C(14)	1.393 (6)
C(16)-C(15)	1.393 (6)	C(17)-C(16)	1.362 (8)
C(18)-C(17)	1.381 (8)	C(19)-C(18)	1.360 (7)
C(2)-C(1)-O(1)	129.1 (4)	C(5)-C(1)-O(1)	125.5 (4)
C(5)-C(1)-C(2)	110.3 (4)	C(3)-C(2)-C(1)	103.0 (4)
C(6)-C(2)-C(1)	111.4 (4)	C(6)-C(2)-C(3)	118.7 (5)
C(4)-C(3)-C(2)	105.7 (4)	C(5)-C(4)-C(3)	102.1 (4)
C(4)-C(6)-C(1)	101.0 (4)	C(13)-C(5)-C(1)	113.9 (4)
C(13)-C(5)-C(4)	125.1 (4)	C(7)-C(6)-C(2)	113.8 (4)
C(8)-C(7)-C(6)	120.0 (5)	C(12)-C(7)-C(6)	121.9 (6)
C(12)-C(7)-C(8)	118.1 (6)	C(9)-C(8)-C(7)	123.8 (7)
C(12)-C(9)-C(8)	117.3 (3)	C(11)-C(10)-C(9)	121.5 (8)
C(12)-C(11)-C(10)	119.8 (3)	C(11)-C(12)-C(7)	119.7 (7)
C(14)-C(13)-C(13)	123.5 (4)	C(15)-C(14)-C(13)	123.7 (4)
C(19)-C(14)-C(13)	119.1 (4)	C(19)-C(14)-C(13)	117.1 (5)
C(16)-C(15)-C(14)	119.4 (3)	C(17)-C(16)-C(15)	121.2 (6)
C(18)-C(17)-C(16)	120.0 (6)	C(19)-C(18)-C(17)	119.3 (6)
C(18)-C(19)-C(14)	122.8 (6)	C(19)-C(18)-C(17)	119.3 (6)

TABLE VII: Bond Lengths (Å) and Angles (Deg) for BpBrBCP

O(1)-C(1)	1.214 (7)	C(8)-C(9)	1.394 (11)
C(1)-C(2)	1.497 (8)	C(9)-C(10)	1.373 (12)
C(1)-C(5)	1.477 (8)	C(10)-C(11)	1.354 (11)
C(2)-C(3)	1.498 (9)	C(11)-C(12)	1.342 (11)
C(2)-C(6)	1.492 (9)	C(13)-C(14)	1.457 (8)
C(3)-C(4)	1.504 (9)	C(14)-C(15)	1.421 (8)
C(4)-C(5)	1.511 (8)	C(14)-C(19)	1.390 (8)
C(5)-C(13)	1.336 (7)	C(15)-C(16)	1.362 (8)
C(6)-C(7)	1.515 (9)	C(16)-C(17)	1.367 (8)
C(7)-C(8)	1.378 (9)	C(17)-C(18)	1.400 (9)
C(7)-C(12)	1.391 (9)	C(18)-C(19)	1.370 (9)
		C(17)-Br(1)	1.873 (6)
O(1)-C(1)-C(2)	125.4 (6)	C(7)-C(8)-C(9)	119.6 (7)
O(1)-C(1)-C(5)	125.7 (6)	C(8)-C(9)-C(10)	121.7 (8)
C(2)-C(1)-C(5)	108.8 (6)	C(9)-C(10)-C(11)	117.3 (8)
C(1)-C(2)-C(3)	104.6 (5)	C(10)-C(11)-C(12)	122.4 (8)
C(1)-C(2)-C(6)	116.2 (5)	C(7)-C(12)-C(11)	121.6 (7)
C(3)-C(2)-C(6)	122.0 (6)	C(5)-C(13)-C(14)	132.2 (5)
C(2)-C(3)-C(4)	108.3 (5)	C(13)-C(14)-C(15)	123.6 (5)
C(3)-C(4)-C(5)	105.5 (5)	C(13)-C(14)-C(19)	119.6 (5)
C(1)-C(5)-C(4)	107.9 (5)	C(15)-C(14)-C(19)	116.8 (5)
C(1)-C(5)-C(13)	120.2 (5)	C(14)-C(15)-C(16)	120.4 (6)
C(4)-C(5)-C(13)	131.7 (5)	C(15)-C(16)-C(17)	122.1 (6)
C(2)-C(6)-C(7)	113.7 (6)	C(16)-C(17)-C(18)	118.6 (6)
C(6)-C(7)-C(8)	121.2 (7)	C(17)-C(18)-C(19)	120.0 (6)
C(6)-C(7)-C(12)	121.4 (6)	C(14)-C(19)-C(18)	122.1 (6)
C(8)-C(7)-C(12)	117.4 (7)	C(16)-C(17)-Br(1)	121.0 (5)
		C(18)-C(17)-Br(1)	120.4 (4)

TABLE VIII: List of Atom Movements for Monomer → Dimer

atom	Δx/Å	Δy/Å	Δz/Å	d/Å
O(1)	0.198	0.341	0.021	0.395
C(1)	0.285	0.406	−0.103	0.507
C(2)	0.181	0.109	0.240	0.320
C(3)	0.199	0.054	0.455	0.500
C(4)	0.176	0.216	0.011	0.279
C(5)	0.467	0.880	−0.593	1.159
C(6)	0.270	0.174	0.344	0.470
C(7)	0.176	0.200	0.372	0.458
C(8)	0.124	0.186	0.492	0.540
C(9)	0.163	0.203	0.580	0.636
C(10)	0.054	0.251	0.577	0.631
C(11)	0.106	0.267	0.537	0.609
C(12)	0.140	0.194	0.471	0.528
C(13)	0.319	1.006	−1.002	1.455
C(14)	0.364	0.558	−0.737	0.993
C(15)	0.198	0.521	−0.762	0.891
C(16)	0.213	0.148	−0.617	0.669
C(17)	0.431	−0.195	−0.470	0.667
C(18)	0.600	−0.168	−0.422	0.753
C(19)	0.595	0.187	−0.556	0.835

TABLE IX: Changes in Cell Dimensions during Conversion

irradn time, h	a, Å	b, Å	c, Å	V, Å^3
		BBCP		
0	31.338 (4)	10.786 (2)	8.687 (1)	2936.3
1	31.334 (4)	10.769 (1)	8.721 (1)	2942.8
3	31.309 (4)	10.757 (2)	8.743 (1)	2944.6
4	31.301 (4)	10.756 (2)	8.744 (1)	2943.9
5	31.290 (4)	10.760 (2)	8.741 (1)	2942.9
6	31.287 (5)	10.764 (2)	8.735 (2)	2941.7
7.5	31.280 (4)	10.771 (2)	8.724 (2)	2939.3
9.8	31.273 (6)	10.786 (2)	8.689 (2)	2930.9
11.1	31.280 (6)	10.790 (3)	8.665 (2)	2924.5
13.6	31.293 (9)	10.806 (8)	8.622 (3)	2915.6
28.6	31.292 (14)	10.809 (8)	8.622 (2)	2915.7
		BpBrBCP		
0	34.227 (5)	10.934 (1)	8.426 (1)	3153
10	34.221 (5)	10.925 (1)	8.441 (1)	3156
20	34.209 (4)	10.914 (1)	8.453 (1)	3156
30	34.197 (5)	10.904 (1)	8.464 (1)	3156
40	34.188 (5)	10.894 (1)	8.474 (1)	3156
50	34.178 (4)	10.884 (1)	8.485 (1)	3156
60	34.165 (4)	10.877 (2)	8.494 (1)	3156
75	34.151 (5)	10.867 (2)	8.508 (1)	3157
105	34.122 (5)	10.843 (2)	8.536 (2)	3158
160	34.093 (8)	10.812 (4)	8.567 (3)	3158

of diolefins.[17] The plane-to-plane separations of 3.60(1) Å for BpBrBCP (compared with 3.80(1) Å for BBCP) suggests that there is a stronger interaction between the molecular pairs in the BpBrBCP crystal.

The structure of the dimer (see Figures 4 and 5) is, as expected, closely related to those of the monomers. The bond lengths and angles in the molecule are normal except that bond C(13)–C(5) is longer than expected and may be an indication of intramolecular strain. In addition, bond lengths in the phenyl ring C(17)–C(12) are shorter than normal and this is probably due to some residual positional scatter in this portion of the molecule simulating high thermal motion.

The nature and size of the atom movements involved can be seen in part in the composite diagram in Figure 6, which shows the relative positions of the monomer and dimer molecules. In Table VIII, we show this in more detail with a list of the actual atom movements. from this we see that, as expected, the largest movements occur for C(5) and C(13), although even the smallest C(4) is still quite significant. The conversions are, in a literal sense, diffusionless.

(b) *Partially Converted Crystals.* As previously mentioned, complete sets of intensity data were recorded for two intermediate points during the converion process. Due to the scheduling of our many experiments, the data collections were necessarily made with different crystals, neither of which were used for the detailed study of cell dimension changes with dimerization.

As a first attempt to find the representative structures for these "mixed" crystals, the procedure adopted for the mixed crystal species 2,5-distyrylpyrazine (DSP–1,4-bis-[2-(2-pyridyl)vinyl]benzene (P2VB)(4:6) was followed.[18]

(17) H. Nakanishi, K. Ueno, and Y. Sasada, *Acta Crystallogr., Sect. B*,34, 2209 (1978).

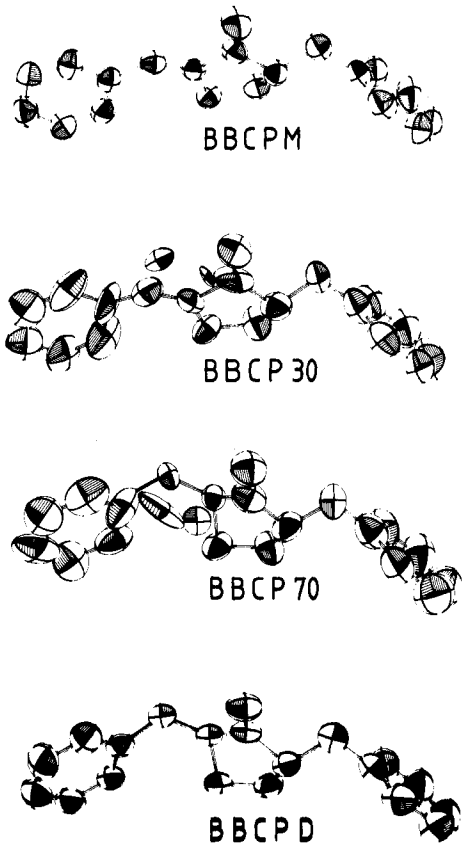

Figure 7. Multiple ORTEP plot showing the monomer and half-dimer equivalent fragments during conversion. The thermal ellipsoids are drawn at the 50% probability level. Unconnected atoms are C(5) and C(13) which belong to the minor components. All views are along [010].

Two sets of coordinates, for the monomer and dimer, were used for each refinement with occupancy factors of x and $(1 - x)$, chosen initially by estimation of the degree of conversion from the cell dimension plots. Each component (i.e., monomer and half-dimer) had its geometry fixed at that found for the pure phases by using the so-called DFIX facility in SHELX, with each set of positions refined in separate blocks. The R values obtained were 0.15 and 0.14 for BBCP30 and BBCP70, respectively, higher than we had hoped for, particularly in view of the successful treatment of the DSP/P2VB system ($R = 0.06$), and several atoms had adopted nonpositive definite temperature factors. Attempts at full-matrix, unblocked refinement failed completely.

In order to investigate the possibility of defining a better structural model we computed F_o syntheses using phases obtained only from atom coordinates for the major component (i.e., monomer for BBCP30 and dimer for BBCP70). On these maps single peaks occurred for all atoms but C(5) and C(13) for which two peaks were obtained with heights corresponding approximately to the estimated composition. Refinment was then attempted with a single set of atom coordinates but with C(5) and C(13) split into two positions with refineable occupancies of x and $(1 - x)$ as before. With anisotropic thermal parameters for all atomic sites, R values of 0.15 and 0.14 were obtained. Final occupancy values for monomer and dimer were 0.64 and 0.36 and 0.35 and 0.65, respectively. Not unnaturally many of the temperature factors show large anisotropic coefficients although there is no indication of a preferred orientation of the vibration ellipsoids, suggesting that there is no single "reaction pathway" direction. In Figure 7, we show the ORTEP plots corresponding to these refinements, along with plots for the monomer and dimer structures. Further attempts to improve the model by representing those atoms with large, very anisotropic thermal parameters by two or three partial atoms sited within the volume covered by the thermal ellipsoids were unsuccessful.

From our results we therefore suggest that these intermediate-phase crystals cannot be represented by a simple, homogeneous solid–solution model. However, this is not to say that the dimerization reaction itself is not homogeneous; we have seen no evidence of phase separation during the reaction. We envisage that, for a given chemical conversion, the concentration of dimer species in the monomer matrix varies in a gradual manner from place-to-place within the crystal, depending on the amount of radiation received. Thus it is plausible to suppose that the outer layers of the crystal will tend to contain a higher percentage of dimer than the core. If this kind of structural model is indeed valid it explains in part the difficulties in achieving a smooth and successful refinement. In the absence of phase separation we are more likely to find a *variety* of molecular orientations intermediate between those of the monomer and dimer since these are likely to depend on the exact local environment. We need, especially, information pertaining to the role of phonons in these solid-state dimerizations.

Clearly, more detailed investigation of these systems is required and such work is currently in hand. It is encouraging to note that, with the particular soild-state dimerizations described here, unlike any other reaction so far described, it has been possible to acquire full X-ray structural data at intermediate levels of conversion. Moreover, the specific atoms involved in the reaction have been directly monitored during the conversion.

Acknowledgment. We acknowledge assistance with data collection provided by Drs. P. Raithby and T. C. McDonnell and Messrs. C. R. Theocharis and T. Abraham. The financial support of the S.R.C. and the Oppenheimer Fund, University of Cambridge, is appreciated.

Supplementary Material Available: Thermal parameters for BBCPM, BpBrBCP, and BBCPD (Tables S1–S3); coordinates and thermal parameters for BBCP30 and BBCP70 (Tables S4–S5); F_o/F_c for BBCPM, BpBrBCP, BBCPD, BBCP30, and BBCP70 (Tables S6–S10); and variation in diffraction intensities during the dimerization of BBCP (Table S11) (45 pages). Ordering information is available on any current masthead page.

(18) H. Nakanishi, W. Jones, and G. M. Parkinson, *Acta Crystallogr., Sect. B.*, **35**, 3103 (1979).